Relevance of a twovariable Oregonator to stable and unstable steady states and limit cycles, to thresholds of excitability, and to Hopf vs SNIPER bifurcations

Kedma BarEli and Richard M. Noyes

Citation: The Journal of Chemical Physics **86**, 1927 (1987); doi: 10.1063/1.452142
View online: http://dx.doi.org/10.1063/1.452142
View Table of Contents: http://scitation.aip.org/content/aip/journal/jcp/86/4?ver=pdfcov
Published by the AIP Publishing

Relevance of a two-variable Oregonator to stable and unstable steady states and limit cycles, to thresholds of excitability, and to Hopf vs SNIPER bifurcations

Kedma Bar-Eli[a] and Richard M. Noyes
Department of Chemistry, University of Oregon, Eugene, Oregon 97403

(Received 18 September 1986; accepted 6 November 1986)

A stiffly-coupled Oregonator model based on the two independent variables Y and Z has been examined in detail with the use of the stoichiometric factor as a single disposable parameter. The trajectories and periods of the stable limit cycles can be generated with unanticipated accuracy from simple linear differential equations. Transitions between stable limit cycles and stable steady states takes place by means of subcritical Hopf bifurcations. Unstable limit cycles and thresholds of excitability can be recovered by integrating the equations of motion backward in time; such procedures cannot be applied so easily for models based on more than two independent variables. We have examined claims of experimental evidence for saddle-node infinite period (SNIPER) bifurcations and have concluded that all currently available evidence is equivocal. Until unambiguous criteria can be established for identifying SNIPER bifurcations in real systems, and until chemical mechanisms have been proposed which generate such bifurcations, observations should be interpreted by existing models based on Hopf bifurcations. Experimental behaviors are listed which can and cannot be simulated in terms of two independent composition variables.

I. INTRODUCTION

In addition to oscillations, the Belousov–Zhabotinsky system can also exhibit the interesting phenomenon of excitability. A specific composition may persist for a long time in an oxidized or in a reduced steady state which is rapidly restored after small perturbations by either silver or bromide ions. However, if either silver-ion addition to a reduced state or bromide-ion addition to an oxidized state exceeds a very sharply defined threshold, then the concentrations of bromide ion and of some other species make excursions of several orders of magnitude before the system returns to its original state. Such a threshold is not a true discontinuity in a mathematical sense, and in principle the magnitude of the final excursion is a continuous function of the initial perturbation. However, our model computations suggest that differences of parts per million in the size of the initial perturbation may cause changes by factors of several thousand in the size of the resulting excursion! This extreme nonlinearity of magnification of the perturbation suggests many analogies to threshold phenomena exhibited by living organisms and other chemical systems.

The possibility of excitability by silver ion of a reduced steady state was first suggested by Field and Noyes[1] after computations with a three-variable Oregonator model. The phenomenon was subsequently observed experimentally by Ruoff,[2] who also observed excitability by bromide ion of an oxidized state[3] and modeled it with an amplified four-variable Oregonator.[4] Noszticzius, Wittmann, and Stirling[5] also report excitability of an oxidized state.

A *threshold of excitability* is a phenomenon observed in an experimental system. In order to model the dynamic behavior of such a system mathematically, we must specify a number of composition variables consisting of concentrations of specified chemical species. All such variables are constrained to finite positive values. If n such variables are sufficient to describe behavior to the desired level of approximation, the state of the system is defined at any time as a point in the bounded positive orthant of a phase space of n dimensions.

The dynamic behavior of such a system is then described by a set of n differential equations which generate a trajectory as the composition of the system evolves with time. Such evolution depends upon the initial state of the system and also upon the values selected for a set of parameters such as rate constants.

For any selected set of parameter values, the entire phase space will contain one or more *basins of attraction*. Such a basin may surround either a locally stable steady state or a stable limit cycle trajectory.[6] If there are two or more such basins of attraction, each will be separated from all others by a separatrix of $n - 1$ dimensions.

A *separatrix* is a mathematical construct consisting of a curve in a two-dimensional phase plane or of a surface in a phase space of three dimensions. Any neighboring point, no matter how close, will initiate a trajectory which eventually leaves the region of the separatrix and moves further into the basin of attraction. In a bounded two-dimensional phase plane, a separatrix may be a closed unstable limit cycle which separates an exterior stable limit cycle from an inner stable stationary state or limit cycle. Alternatively, the separatrix may be a curve extending between two points on the accessible limits of the phase plane.

A separatrix somewhat resembles but is not identical to a threshold of excitability such as is observed in the experimental system. Thus, the threshold exists entirely within a single basin of attraction and is not a true discontinuity in the mathematical sense appropriate to a separatrix.

[a] Department of Physical Chemistry, University of Tel-Aviv, 69978 Ramat-Aviv, Tel-Aviv, Israel.

 0021-9606/87/041927-11$02.10

As parameter values are changed, the nature of the phase space may also change, and basins of attraction may merge or separate discontinuously with the simultaneous destruction or creation of a separatrix. Thus, in a subcritical Hopf bifurcation, a locally stable steady state will disappear discontinuously and become part of the basin of attraction of a pre-existing stable limit cycle; a separatrix is simultaneously destroyed. If the Hopf bifurcation is supercritical, a stable limit cycle will grow from the pre-existing stable steady state, but no separatrix will be created or destroyed.

In general, it is difficult to determine the location of a separatrix in a space of n dimensions containing two or more basins of attraction. If trajectories from two different initial points move into different basins, the separatrix passes between them. However, it is very cumbersome to define a surface by examining trajectories calculated from many different initial points. If one tries to integrate trajectories backward in time, they are likely to leave the region of phase space which has physical meaning, and they may do so before they have even come close to the separatrix.

For the special case of $n = 2$, the separatrix may be an unstable limit cycle which separates a locally stable steady state or limit cycle from a surrounding locally stable limit cycle. For this special case, a trajectory integrated backward in time will converge upon the separatrix and define its location. Such a procedure is not easily available in a phase space of more than two dimensions.

The above principles are illustrated in this paper with a stiffly coupled Oregonator model for which variation of the stoichiometric factor as the single disposable parameter permits an approximate modeling of several experimental phenomena by means of motions in a phase plane. The model is presented in Sec. II. In Sec. III, we discuss the nullclines whose intersections define all steady states whether stable or unstable. In Sec. IV, we discuss the stable limit cycles which occur within a specific range of values of the stoichiometric factor. In Sec. V, we discuss the unstable limit cycles which may separate locally stable steady states and stable limit cycles generated by identical values of the stoichiometric factor. In Sec. VI, we discuss the use of this model to simulate the excitability of both reduced and oxidized steady states in real systems.

Subcritical Hopf bifurcations are the only kinds possible with this approximate model. Noszticzius *et al.*[5] have claimed that experimental evidence is also consistent with an alternative interpretation of observed bifurcations. In Sec. VII, we examine the problem of using experimental data to determine the appropriateness of specific mathematical models for description of experimental observations.

In Sec. VIII, we examine the extent to which the approximate model in two variables suffices to simulate experimental observations and the ways in which other behavior could be accommodated.

This organization has been developed because we did not believe the arguments in Secs. VI and VII could be appreciated without a prior description of the possible bifurcations between stable and unstable steady states in this model. Those bifurcations have previously been examined by Tyson[26,27] and by Rinzel and Troy.[7,8] The arguments we use rely heavily on numerical computations and differ somewhat from the more analytical procedures employed previously. However, several of our conclusions have been anticipated by the prior work. We shall try to indicate such situations below.

II. THE BASIC MODEL

The regular Oregonator[9] model consists of coupled differential Eqs. 1–3 where the parameters f, A, and k_1–k_5 are positive constants. Application to chemical systems assumes $A \equiv [BrO_3^-]$, $X \equiv [HBrO_2]$, $Y = [Br^-]$, and $Z \equiv [Ce(IV)]$.

$$\frac{dX}{dt} = k_1AY - k_2XY + k_3AX - 2k_4X^2, \tag{1}$$

$$\frac{dY}{dt} = fk_5Z - k_1AY - k_2XY, \tag{2}$$

$$\frac{dZ}{dt} = k_3AX - k_5Z. \tag{3}$$

In order to reduce the number of independent variables to two, we adopt the approximation that $dX/dt = 0$ at all times.[10] Then we obtain Eq. (4) as the only positive solution for $X(Y)$. It is convenient to write many of the subsequent equations in terms of X as though it were an independent variable; it is important to remember that X is actually a unique function of Y.

$$X(Y) = \frac{k_3A - k_2Y + \sqrt{(k_3A - k_2Y)^2 + 8k_1k_4AY}}{4k_4}. \tag{4}$$

It is proved in Appendix A that for any set of parameter values Eqs. (1)–(4) lead to one and only one point (Y_{ss}, Z_{ss}) in the positive quadrant of the YZ plane such that $dY/dt = dZ/dt = 0$. Therefore, on the bounds of the accessible regions of that plane all points will initiate trajectories directed into the same basin of attraction. That basin will surround either the steady state itself or the outermost of any stable limit cycles around it.

If we let $y = Y - Y_{ss}$ and $z = Z - Z_{ss}$ and linearize the equations in the neighborhood of this steady state, we obtain secular Eq. (5) where the quantities a–d are defined in Eqs. (6)–(9):

$$\begin{vmatrix} a-\omega & b \\ c & d-\omega \end{vmatrix} = 0, \tag{5}$$

$$a = \left(\frac{\partial \dot{y}}{\partial y}\right)_z = -k_1A - k_2X_{ss} - k_2Y_{ss}\left(\frac{dX}{dY}\right)_{ss}, \tag{6}$$

$$b = \left(\frac{\partial \dot{y}}{\partial z}\right)_y = fk_5, \tag{7}$$

$$c = \left(\frac{\partial \dot{z}}{\partial y}\right)_z = k_3A\left(\frac{dX}{dY}\right)_{ss}, \tag{8}$$

$$d = \left(\frac{\partial \dot{z}}{\partial z}\right)_y = -k_5. \tag{9}$$

The roots of the secular equation are defined by

$$\omega = \frac{a + d \pm \sqrt{(a+d)^2 - 4(ad - bc)}}{2}. \tag{10}$$

If $(a+d)^2 > 4(ad - bc)$, both roots are real. Because

TABLE I. Values selected for parameters.

k_1A	0.2
k_2	2×10^9
k_3A	1000
k_4	5×10^7
k_5	1

the accessible phase plane is bounded, arguments developed previously[12] and the fact there is only one steady state in the positive YZ quadrant lead to the requirement that for this model $ad - bc > 0$ and both real roots have the same sign, which is that of $a + d$. If $a + d < 0$, the steady state is a stable node; if $a + d > 0$, the node is unstable.

When $(a + d)^2 = 4(ad - bc)$, the two real roots become equal. When $(a + d)^2 < 4(ad - bc)$, the roots are complex conjugate and the steady state is a focus which is stable or unstable depending upon the sign of $a + d$. Because the accessible phase plane is bounded, the Poincaré–Bendixon theorem requires that an unstable node or focus is always surrounded by at least one stable limit cycle.

When $a + d = 0$, the system undergoes a Hopf bifurcation as it makes a transition between stable and unstable foci. If that bifurcation is supercritical, the associated stable focus is globally attracting. If the bifurcation is subcritical, the associated stable focus is surrounded by a stable limit cycle.

The computations reported here used the set of parameter values in Table I. That set has been used previously. Only after most of the computations had been completed did we become aware of the analysis of experimental data by Field and Försterling[13] which suggests a modified set might have been preferable. The analysis of critical ratios by Tyson[14] indicates the qualitative behavior should not be seriously affected by the use of appropriately revised rate constants.

TABLE II. Behaviors obtained with different values of f.

	Globally attracting stable node
10.538	
	Globally attracting stable focus
1.947 5	
	Stable focus and stable limit cycle separated by unstable limit cycle
1.755 815	Subcritical Hopf bifurcation surrounded by stable limit cycle
	Unstable focus surrounded by stable limit cycle
1.425 271	
	Unstable node surrounded by stable limit cycle
0.505 031	
	Unstable focus surrounded by stable limit cycle
0.500 055 0[a]	Subcritical Hopf bifurcation surrounded by stable limit cycle
	Globally attracting stable focus
0.495 029	
	Globally attracting stable node

[a] We have made no effort to define the very narrow range of f values within which unstable and stable limit cycles both surround the locally stable focus with $f < 0.500\,055\,0$.

The global behavior of the system is then determined by the value of the single parameter f. Table II shows the ranges within which different types of behavior will occur. Limit cycle and excitability behaviors are developed in more detail below.

III. BEHAVIOR OF NULLCLINES

For any value of Y, the value of Z at which Eq. (3) is zero is given by

$$Z(Z_{\text{null}}) = k_3AX/k_5 . \tag{11}$$

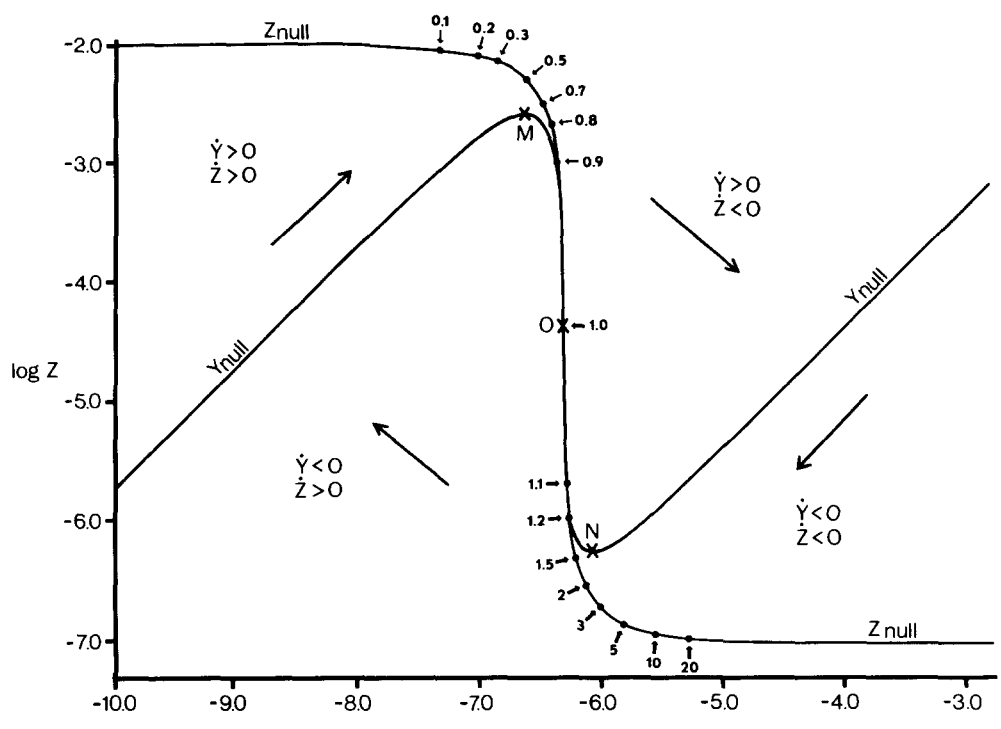

FIG. 1. Logarithmic plot of nullclines for $f = 1$ and parameter values of Table I. The major fields of the figure designate signs of $\dot{Y}$ and $\dot{Z}$, and major arrows indicate quadrants into which trajectories are directed in those fields. The nullclines intersect at steady-state point O. Crosses designate O and also the relative maximum of Y_{null} at point M and the relative minimum at point N. If f deviates from unity, the Y nullcline will be shifted vertically by $-\log f$, and the point of intersection with the Z nullcline will also shift. Small arrows to points and accompanying numbers designate the steady-state compositions for the indicated values of f. Approximate equations which generate these nullclines are developed in Appendix B.

This Z nullcline is designated Z_{null} in the logarithmic plot of Fig. 1 for the parameter values of Table I. The same curve is obtained for all values of f.

The Y nullcline along which Eq. (2) is zero is given by

$$Z(Y_{\text{null}}) = (k_1AY + k_2XY)/fk_5 . \quad (12)$$

This curve is also plotted for $f = 1$ in Fig. 1. The intersection of the two nullclines is the steady state for this value of f.

Because $Z(Y_{\text{null}})$ is inversely proportional to f, the Y nullcline for any other value of f will be obtained by shifting the curve in Fig. 1 vertically by a constant increment of $-\log f$. Small arrows are used for different values of f between 0.1 and 20 in order to designate the steady states calculated as described in Appendix A.

Approximate (but very nearly exact) analytical expressions for the nullclines of Fig. 1 are developed in Appendix B. Those expressions indicate that the steady state will coincide with the local maximum in the Y nullcline (point M) when $f = 0.500\,010$ and will coincide with the local minimum (point N) when $f = 2.414$.

The argument developed in Ref. 12 points out that the local stability of the steady state is determined by the angles at which the nullclines intersect. Because $Z(Z_{\text{null}})$ is a monotonically decreasing function of Y, the argument shows that a necessary but not sufficient requirement for an unstable steady state is that $dZ(Y_{\text{null}})/dY < 0$ at the intersection of the nullclines. The conclusion of Table II is that locally unstable steady states lie in the range $0.500\,055\,0 < f < 1.775\,815$. This entire range does indeed lie in the range between the local maximum and the local minimum in the Y nullcline.

IV. BEHAVIOR OF STABLE LIMIT CYCLES

Table II shows that all stable (and unstable) limit cycles can occur only in the range of $0.500\,05 < f < 1.9475$. Figure 2 shows plots of limit-cycle trajectories for $f = 0.505$ (designated by subscripts 1) and for $f = 1.940$ (designated by subscripts 2); those trajectories span most of the range within which limit cycles are possible.

The trajectories in Fig. 2 are virtually indistinguishable from projections in the YZ plane of the three-dimensional trajectories obtained by abandoning the approximation of Eq. (4). If new rate constants were selected on the basis of the suggestions of Field and Försterling,[13] values of X would probably be increased at some stages and those of Y decreased even though qualitative behavior would remain much the same.

The major conclusion from Fig. 2 is that stable limit cycles change very little over the entire range of f values for which they are possible. The maximum values of Z designated M_1 and M_2 are inversely proportional to f and occur very near to but not identical with the local maximum in the Y nullcline. The broad minima in Z are lumped under an N designation and are not sharply defined; they must lie on trajectories which pass below the local minimum in the Y nullcline. Maximum values of Y at P_1 and P_2 are almost independent of f, while minimum values of Y at Q_1 and Q_2 are approximately proportional to f. Of course the steady states O_1 and O_2 must lie inside the relevant limit cycles, but

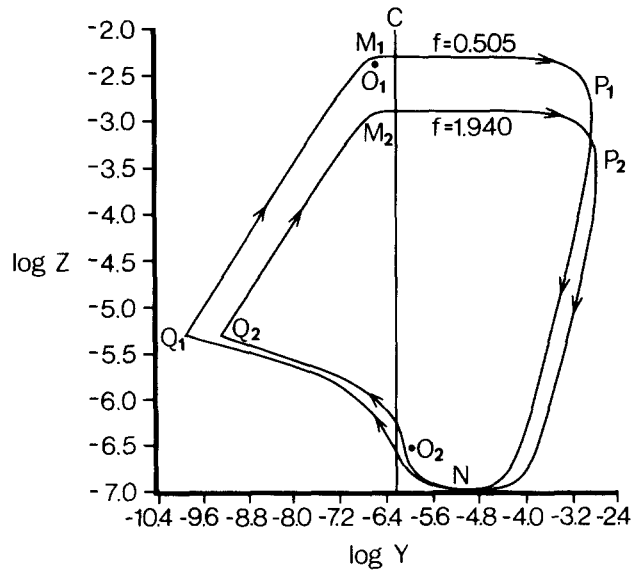

FIG. 2. Stable limit cycles for $f = 0.505$ (designated by subscripts 1) and for $f = 1.940$ (designated by subscripts 2). Points M, P, and Q indicate maximum Z and maximum and minimum Y, respectively. The broad minimum in Z is designated N without any effort to define a specific point. Vertical line C at $Y = Y_{\text{crit}}$ is used to show where the approximate equations of Appendix B change discontinuously. Point O_1 indicates a steady state at $Y = 2.525\times10^{-7}$, $Z = 4.950\times10^{-3}$; and point O_2 indicates a steady state at $Y = 7.350\times10^{-7}$, $Z = 3.128\times10^{-7}$. Appendix C shows how the trajectories in this figure follow from Eqs. (1)–(4) and the nullcline analysis of Fig. 1 and Appendix B.

they span almost the entire range from the top to the bottom of the limit cycles in Fig. 2.

The approximate analysis of nullclines in Appendix B suggests that X may be assigned one of two constant values which change virtually discontinuously whenever Y passes through Y_{crit} indicated by line C in Fig. 2. Appendix C shows that this major approximation still permits very good estimates for the extrema and for the periods of the limit cycles in Fig. 2.

For the parameter values of Table I, the oscillations are of relaxation type. Thus, the transition from $Z_{\max}$ at point M to $Y_{\max}$ at point P takes only about 1.5 s during a total period of over 20 s, and the transition from Y_{crit} (line C near point N) to $Y_{\min}$ at point Q takes less than 10^{-3} s. Other sets of rate-constant parameters might generate oscillations for which the relaxations were less sharp and which might even approximate sinusoidal behavior.

The approximate analysis of Appendix C also concludes that the period of limit cycle oscillations should be almost independent of the parameter f. The exact integrations of the trajectories support that prediction. The minimum period of 21.7 s was found when f was about 0.9. It increased in either direction as f approached the bifurcation limit, but the period was only 24.6 s at $f = 1.940$ and was 22.6 s at $f = 0.5001$.

It appears that if this model with the parameter values of Table I generates any limit cycle oscillations, they are of large amplitude and pass outside the local extrema M and N in the Y nullcline. Small-amplitude limit cycles are conspicuously missing from our computations for this model. That

result is consistent with the conclusion of Tyson[27] and of Troy[8] that for these parameter values any Hopf bifurcations will be subcritical rather than supercritical. This result can also be obtained by methods discussed by Hassard, Kazarinoff, and Wan.[28]

V. BEHAVIOR OF UNSTABLE LIMIT CYCLES

Table II indicates that at $f = 1.755\,815$ there is a subcritical Hopf bifurcation, and for all larger values of f the steady state is locally stable. However, until $f = 1.9475$ a stable limit cycle is also possible. Between these limiting values of f, there must be a separatrix consisting of an unstable limit cycle such that points on one side initiate trajectories which decay to the steady state, and points on the other side grow to the stable limit cycle.

This kind of behavior was anticipated by Tyson[27] and was also recognized and modeled by Janz, Vanecek, and Field.[15] They used a model with more than two independent variables and comment that they could not define the unstable limit cycle by integrating backward in time. Rinzel and Troy[7] have also discussed a situation very similar to the one presented here.

A major advantage of a model restricted to two variables like ours is that it is comparatively simple to generate an unstable limit cycle as the closed curve approached by integrating the equations of motion backward in time. Figure 3 presents a number of unstable limit cycles calculated in this way. It is worth noting that the unstable trajectory for $f = 1.940$ employs precisely the same f value as one of the stable limit cycle curves in Fig. 2 and is of course associated with the same steady state.

As f increases from the Hopf bifurcation, the unstable limit cycles grow slowly at first but then expand very rapidly until they intersect and destroy the exterior stable limit cycle.

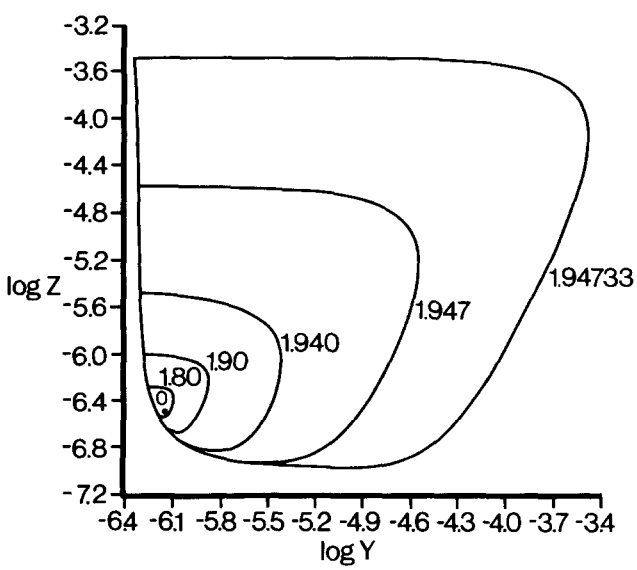

FIG. 3. Unstable limit cycles for different f values. A point inside one of these curves will initiate a spiral trajectory which decays to a steady state which is a stable focus. A point outside will go to a stable limit cycle like those shown in Fig. 2. Point O is the locally-stable steady state associated with the unstable limit cycle for $f = 1.940$; it is identical with point O_2 in Fig. 2.

For the f values chosen in Figure 3, the Y and Z nullclines almost coincide in the left part of the figure with the Y nullcline slightly to the left. A trajectory initiating very close to but to the left of that nullcline will cross it as it rises but will almost simultaneously cross the Z nullcline and eventually spiral into the steady state.

Another Hopf bifurcation occurs at $f = 0.500\,055\,0$. We established that we could generate stable large-amplitude oscillations for f values slightly less than this, so this bifurcation is also subcritical. However, simultaneous stable limit cycles and steady states seemed to be possible for a range of f values of only a few parts per million. We did not find it practicable to try to define unstable limit cycles in such a narrow range. Our conclusions are consistent with those reached previously by Tyson[27] and by Troy.[8]

VI. EXCITABILITY OF STABLE STEADY STATES

One of the more interesting behaviors of this model is the phenomenon of excitability. Such possibilities for both large and small values of f were noted by Tyson.[27] If f is increased slightly above the maximum value shown in Fig. 3, the steady state will become a globally stable basin of attraction and all trajectories will eventually decay to it. However, the former separatrix of the unstable limit cycle to the left of and very close to the Y nullcline will become a threshold of excitability having somewhat similar properties. A perturbation of the steady state which leaves Y still above the threshold will initiate a trajectory which rapidly returns to the steady state. A perturbation which drives Y even very slightly below the threshold will initiate an excursion which follows much of the trajectory of the stable limit cycles of Fig. 2 before the ultimate decay.

Figure 4(a) shows the starts of two trajectories initiated by decreasing Y from the steady-state value at constant $Z = Z_{ss}$. The perturbation necessary to initiate trajectory 2 was less than 0.01% greater than the perturbation necessary to initiate trajectory 1. A full plot of trajectory 1 would require a field very few times that of Fig. 4(a). A full plot of trajectory 2 on the same linear scale would require a field with an area of several square meters even for the dimensions of the reproduction of Fig. 4(a) in this journal!

Figure 4(b) shows logarithmic plots of full trajectories initiating very much like trajectory 2 in Fig. 4(a). The generation of Fig. 4(b) illustrates the advantages of the two-variable model of this paper. It was virtually impossible to select perturbations of the steady state which could generate the different trajectories shown. Instead, various points were selected on the Y nullcline. Each such point was integrated forward in time to generate the trajectory for decay to the steady state. The same point was also integrated backward in time to generate the trajectory which would have led to that point. At least trajectories 1–3 in Fig. 4(b) would have been initiated by perturbations intermediate between those initiating trajectories 1 and 2 in Fig. 4(a)!

Figures 5(a) and 5(b) show that excitability by increasing Y can also be generated for a steady state with f near 0.5. The linear plot in Fig. 5(a) shows two almost identical per-

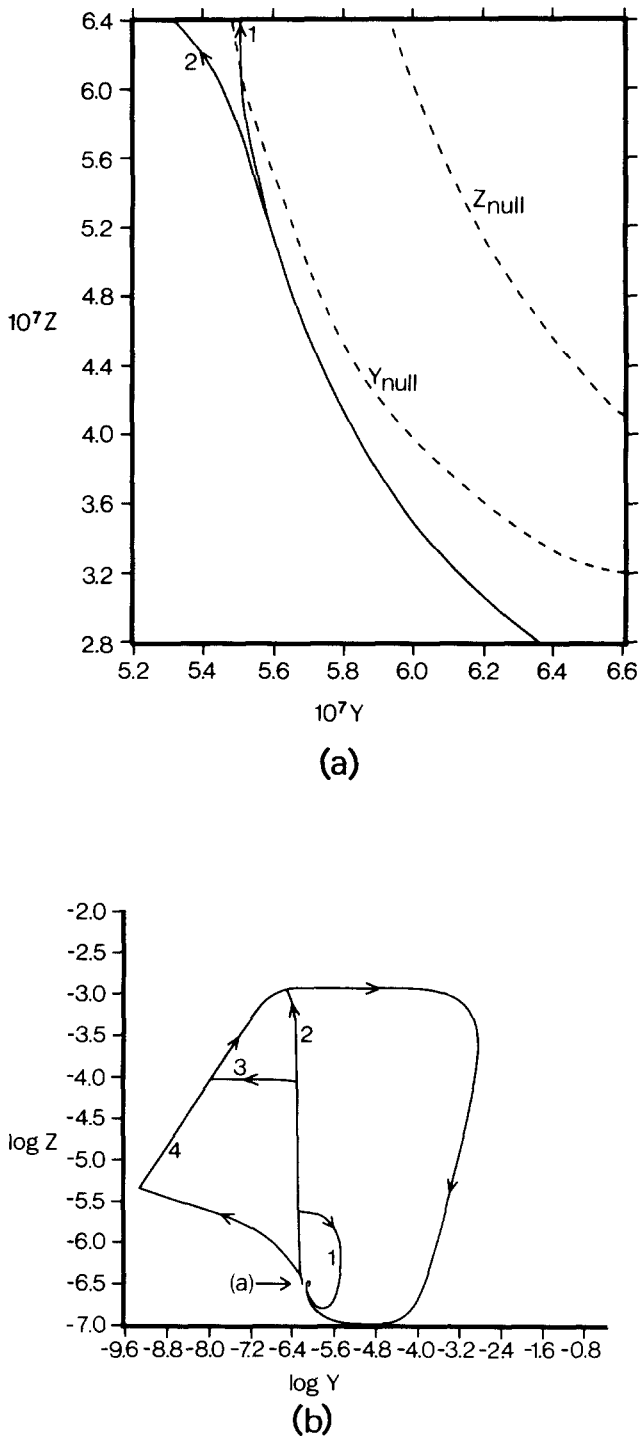

FIG. 4. (a) Linear plot illustrating sharpness of threshold of excitability for a system with $f = 2.106\,985$ which generates a globally stable steady state at $Y_{ss} = 7.767 \times 10^{-7}$, $Z_{ss} = 2.807 \times 10^{-7}$. Dashed curves show the nullclines which intersect at that steady state. Trajectories 1 and 2 were initiated by discontinuously decreasing Y from the steady-state value while maintaining Z constant at Z_{ss}. Trajectory 1 was initiated at $Y_0 = 6.3779 \times 10^{-7}$; it crosses the Y nullcline within the field of the figure and will rise to cross the Z nullcline before continuing the spiral decay to the steady state. Trajectory 2 was initiated at $Y_0 = 6.3778 \times 10^{-7}$. It is diverging from the Y nullcline as it leaves the field of the figure and will rise to Z about 1.2×10^{-3} and then increase Y to about 1.4×10^{-3} before it also decays by spiraling to the same steady state. (b) Logarithmic plots of four trajectories initiated by almost identical perturbations of Y from the steady state for $f = 2.106985$. All trajectories eventually decay to that steady state but first undergo major excitability. The arrow indicates the location of the small region shown in (a).

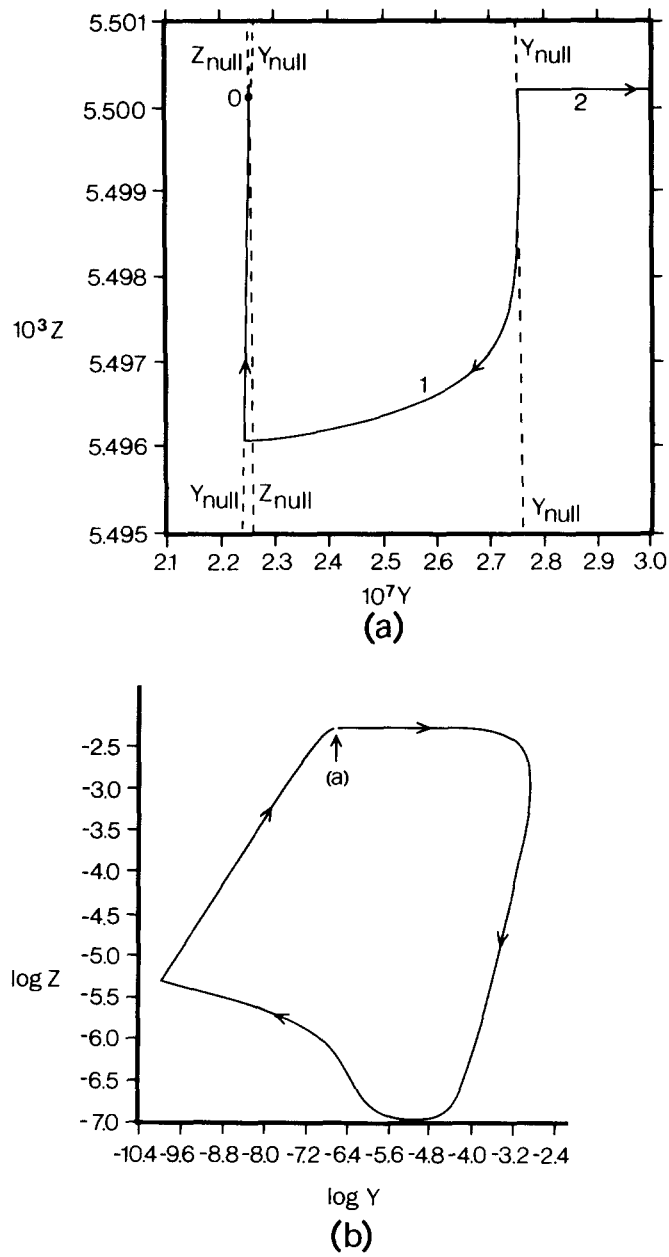

FIG. 5. (a) Linear plot illustrating threshold of excitability for a steady state with $f = 0.45$. The steady state is $Y_{ss} = 2.249\,959 \times 10^{-7}$, $Z_{ss} = 5.500\,164 \times 10^{-3}$. The Y and Z nullclines are designated with dashed curves which intersect at the steady state. The two segments of the Y nullcline are arms of an inverted parabola. Trajectory 1 was initiated by perturbing Y to $2.751\,249 \times 10^{-7}$; it returns to the stable node after a brief excursion. Trajectory 2 was initiated by perturbing Y to $2.751\,474 \times 10^{-7}$; it rapidly leaves the region of the steady state. (b) Logarithmic plot of full trajectory whose initiation is designated 2 in (a). The arrow indicates location of the small region shown in (a).

turbations which lead to very different behavior. Trajectory 1 does not quite attain the threshold of excitability, which is to the right of but virtually identical with the Y nullcline; the system rapidly decays to the globally attracting stable node. Trajectory 2 is initiated by a perturbation which goes beyond the threshold, and the system leaves on a major excursion shown in the logarithmic plot of Fig. 5(b).

Linear Fig. 6 illustrates the excitability thresholds for

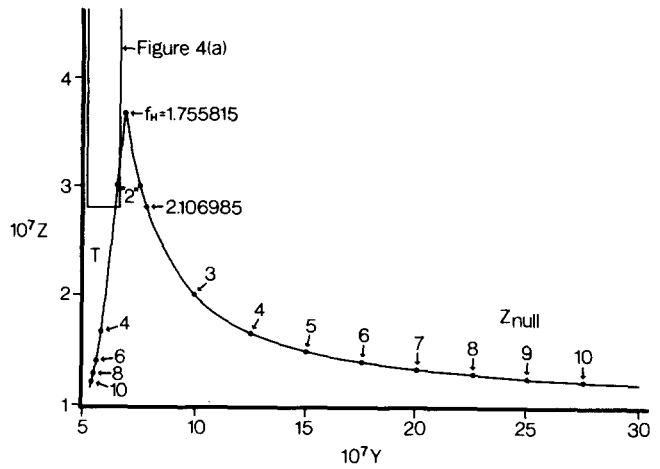

FIG. 6. Linear plot of excitability thresholds at large f. The curve marked Z_{null} is the Z nullcline for f greater than the f_H value of 1.755 815 for the Hopf bifurcation; it can be compared with the logarithmic plot in Fig. 1. The curve marked T is the threshold of excitability if Y were perturbed from the steady state at constant Z. Points designated by arrows are the steady states and thresholds for the indicated values of f. The field of the figure begins at Y_{crit}. The box in the upper left-hand corner marks the limits of the lower part of the field of Fig. 4(a) and permits that figure to be related to what would happen with other values of f.

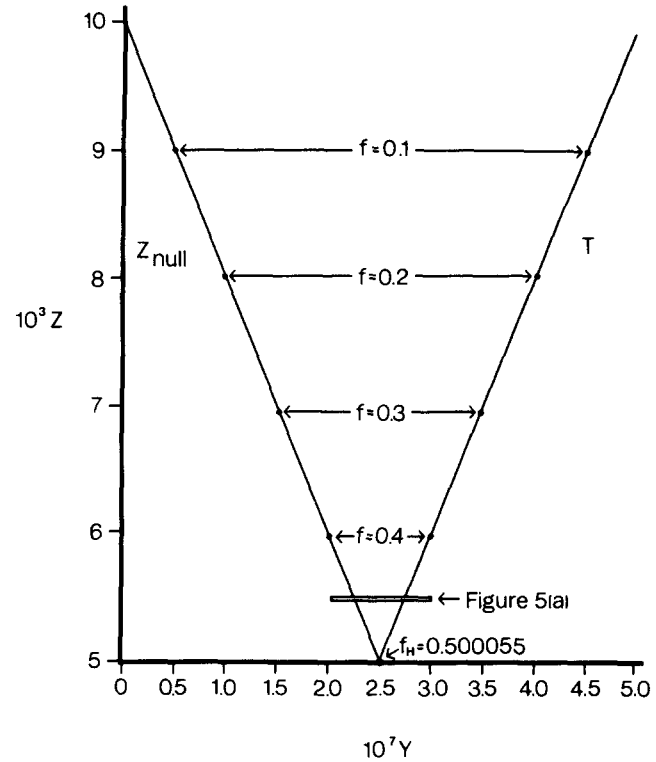

FIG. 7. Linear plot of Z_{null} and thresholds of excitability at small f. The meanings of the curves are similar to those in Fig. 6. The f_H designation is for the Hopf bifurcation at 0.500 055. The field of the figure is from 0 to Y_{crit}. The small box in the region appropriate for $f = 0.45$ marks the limits of the field of Fig. 5(a).

stable steady states with large values of f. Two curves in that figure diverge from the steady state at the Hopf bifurcation when $f_H = 1.755\,815$. At smaller values of f, steady states are locally unstable and are surrounded by stable limit cycles.

One of the curves in Fig. 6 is a portion of the Z nullcline whose more extended behavior is shown in logarithmic Fig. 1. Along this nullcline, arrows are used to designate steady states for different values of f.

The curve T diverges from the Z nullcline at f_H. If $f_H < f < 1.9475$, a point on T represents a point on the separatrix of an unstable limit cycle like those in Fig. 3. If the steady state at any value of f were perturbed at constant Z to go beyond curve T, the resulting trajectory would go to a stable limit cycle.

If $f > 1.9475$, a point on T represents a threshold of excitability along which a perturbation from Y_{ss} to Y_T at constant Z will initiate a major excursion before a return to the globally-stable steady state. The curve T seems to be continuous as it passes through $f = 1.9475$. As f becomes indefinitely large, Y_T will approach the Y_{crit} value of 5×10^{-7}.

As is shown in Appendix B, X is nearly constant along the Z nullcline in Fig. 6, and to this approximation Eq. (A2) demonstrates that Y_{ss} is directly proportional to f. The excitability threshold Y_T never deviates much from the Y value at the Hopf bifurcation, so to a fair approximation

$$(Y_{ss} - Y_T)/Y_{ss} = (f - f_H)/f. \tag{13}$$

This approximation is valid to within 10% at $f = 2$ and within 2% at $f = 12$.

Similar Fig. 7 illustrates excitability thresholds for stable steady states with small values of f. As f approaches zero, Y_T will also approach Y_{crit} for these plots.

As can be inferred from Eq. (B4) in Appendix B, the Y nullcline in this region is an inverted parabola passing through the origin of composition space with axis almost coincident with Y_{ss} at the Hopf bifurcation. Then to an excellent approximation the points in Fig. 7 for any value of f lead to

$$(Y_T - Y_{ss})/Y_{ss} = 2(f_H - f)/f. \tag{14}$$

This approximation is valid to better than 0.1% for $f < 0.4$.

VII. HOPF VS SNIPER BIFURCATIONS

The two-variable model as developed above assumes a specific set of rate constants and leaves one disposable parameter f which is constant independent of composition along a particular trajectory. When f is either small or large, the model generates a stable steady state. When f is small, Z_{ss} is large and the model is simulating an experimental system in an oxidized state. When f is large, Z_{ss} is small and the equivalent experimental system is in a reduced state. A range of intermediate f values will generate limit cycle oscillations.

For this model, transitions between oscillations and stable steady states take place in the neighborhood of subcritical Hopf bifurcations.

Maselko[16] has discussed other types of bifurcations in systems of two variables such that a stable limit cycle and a stable steady state can undergo discontinuous transformations. The other type of importance to this paper is called a saddle-node infinite period (SNIPER) bifurcation.

The arguments presented by Maselko are primarily topological. Even when the composition plane has a globally

attracting stable node or focus, a saddle point and an unstable steady state are also present. If change of parameters causes the stable node and the saddle point to coalesce, behavior at the bifurcation will make a discontinuous transition to a stable limit cycle around the unstable steady state. The reverse transition from the limit cycle will take place without hysteresis but with an indefinite lengthening of the period of that cycle; hence the IPER in SNIPER.

Maselko[16(a)] made a detailed study of a Belousov–Zhabotinsky system with malic acid substrate in a flow reactor and interpreted the behavior to involve a SNIPER bifurcation. Noszticzius, Stirling and Wittmann[17] subsequently made a similar assertion about an oxalic acid system from which bromine was being removed by a stream of gas whose flow rate could be varied. Gaspár and Galambosi[18] studied the same reaction in a CSTR. Finally, Noszticzius, Wittmann, and Stirling[5] have indicated that with the customary malonic acid substrate the transition from induction period to oscillations may take place by way of a SNIPER bifurcation.

There is a complete agreement that as experimental conditions change a *B–Z* system may make virtually discontinuous transitions between a stable steady state and large-amplitude oscillations. It may be dangerous to assign those transitions to models, be they Hopf or SNIPER, based on mathematical equations involving only two independent variables. However, it is useful to examine the types of evidence from which such assignments have been made:

(1) Noszticzius *et al.*[5] have claimed that excitability during the induction period of a malonic acid system is evidence for a SNIPER bifurcation.

(2) In principle, a subcritical Hopf bifurcation would exhibit hysteresis when transitions were made in opposite directions, while a SNIPER bifurcation would not exhibit hysteresis.

(3) As a system underwent a transition from limit cycle to globally stable steady state, the period of the limit cycle would become indefinitely long for a SNIPER bifurcation but would remain finite for a Hopf bifurcation.

(4) Only one steady state (locally stable or unstable) is involved in a Hopf bifurcation while three and one exist on opposite sides of a SNIPER bifurcation. However, even when three steady states existed, only one would be experimentally observable.

We do not believe that the excitability criterion (1) is useful for determining type of bifurcation. Noszticzius *et al.*[5] are correct in stating that as a steady state approaches a SNIPER bifurcation the system will exhibit excitability with a steadily decreasing perturbation needed to attain the threshold. However, *precisely* the same behavior is exhibited in Sec. VI above for the approach to either of the subcritical Hopf bifurcations in our model. In fact, for our model *every* globally-stable steady state is potentially excitable.

The Noszticzius[5] observations were made for a malonic acid substrate in the induction period. Such a system is in an oxidized steady state corresponding to a small f in our model. As the induction period continues, more and more bromomalonic acid (BrMA) is produced, and this production has the effect of increasing f. When f has increased to very slightly more than 0.5, the more and more excitable steady state will jump to full-amplitude oscillations just as is observed by Noszticzius *et al.*

The hysteresis criterion (2) appears to be little more valuable for determining type of bifurcation from experimental observation. For our model with small f, we showed in Sec. V that the hysteresis at the Hopf bifurcation is measured in parts per million of the control parameter and would be impossible to observe; this is precisely the circumstance for the bifurcation being studied by Noszticzius.

The discussion in Sec. V did indicate a possible hysteresis of the order of 10% in f for a bifurcation at large f corresponding to a reduced state. Such hysteresis might be detected experimentally with difficulty. Detection would provide evidence for a Hopf bifurcation; absence of detection could not confidently be considered evidence for a SNIPER bifurcation.

The period-lengthening criterion (3) is also ambiguous, at least in reactors subject to a flux of matter. For our model in a closed system, the computations in Sec. IV report little change of period as a discontinuity is approached by an oscillatory system. In contrast, some experimental observations[16–18] detect major increases of period before oscillations cease. However, we believe that all of these observations were made on systems subject to flow of fresh reactants or of gas to sweep out bromine.

We have examined behavior of our model if A remains constant but CSTR flow terms are added to Eqs. (1)–(3). Those flow terms are of the form $-k_0X$, $k_0(Y_0 - Y)$, and $k_0(Z_0 - Z)$. Of course Eq. (4) should be modified by a trivially small amount to include the flow term in the coupling of X to Y. Figure 8 shows a dramatic increase in period as the Hopf bifurcation near $f = 0.74$ is approached. The behavior in our Fig. 8 looks very much like that of one of the curves of Fig. 3 in Ref. 17. This rapid lengthening of period near a Hopf bifurcation in a model system containing flow terms casts suspicion on efforts to use experimental observation of period increase as evidence for SNIPER bifurcations.

The number of steady states criterion (4) does not lend itself to direct experimental test because two of the three states in the SNIPER model are not observable. As is shown

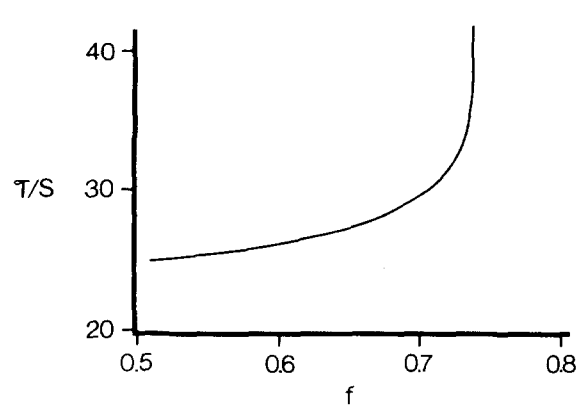

FIG. 8. Behavior of limit cycle period τ with changing f when flow terms are added to the model of Sec. II. The computations used $Y_0 = 1\times10^{-5}$, $Z_0 = 1\times10^{-4}$, $k_0 = 4.5\times10^{-3}$. Hopf bifurcations were near f values of 0.51 and 0.74.

in Appendix A, the model developed in this paper generates only one steady state and is therefore inconsistent with a SNIPER model. If the parameter f were made a function of the composition variables Y and Z, the model could undoubtedly be made to generate three or even five steady states; we do not presently see any need for such treatments.

Our conclusion from this analysis is that *as of now there is no experimental evidence which unequivocally supports a SNIPER bifurcation*. Until there is more convincing evidence, or until a chemical mechanism capable of generating a SNIPER bifurcation has been proposed, we believe it is appropriate to invoke Ockham's razor[19] and to explain observations by means of the Hopf bifurcation which involves a single steady state and which can be generated by known chemical reactions.

VIII. DISCUSSION

The Belousov–Zhabotinsky system undoubtedly exhibits the richest phenomenology of any known nonliving collection of chemicals. Even if we ignore complexities like wave phenomena[20,21] and coupling of flow reactors[22–24] and restrict our attention to systems consisting of a single uniform solution, the following phenomena have been claimed to occur:

(i) excitability of reduced steady states,
(ii) excitability of oxidized steady states,
(iii) limit-cycle relaxation oscillations,
(iv) bifurcations between limit cycles and both reduced and oxidized steady states,
(v) bistability in a flow reactor,
(vi) temporary bistability in a closed system,
(vii) bursting with alternating trains of large-amplitude and small-amplitude oscillations,
(viii) chaotic irregular combinations of bursting sequences.

The model selected for this paper is a stiffly coupled Oregonator which employs a constant stoichiometric factor for trajectories of a specific system and which assumes that all states of the system can be described in terms of two independent variables Y and Z. This restriction to two variables offers a major advantage in that integration backward in time will generate convergence on unstable limit cycles and thresholds of excitability. If more than two independent variables were used, backward trajectories would diverge and be difficult to calculate.

However, restriction to two variables is of necessity an approximation. As discussed above, that approximation is capable of simulating the excitabilities (i,ii), oscillations (iii), and bifurcations (iv) of the features mentioned above. Hopf bifurcations are the only kind which can be obtained with this simple model because it generates a single steady state.

We have not specifically tried to use this model to generate bistability (v). However, we have little doubt such generation would be possible as a result of the robust bistability obtained by De Kepper and Bar-Eli[25] with a slightly more complicated Oregonator model.

This two-variable model is much less satisfactory for simulating behaviors (vi) to (viii) listed above.

Ruoff[4] did simulate temporary bistability (vi) with an amplified Oregonator model having no stoichiometric factor but seven irreversible rate constants instead of the five in Table I. That model also had four independent variables, but we believe most of the qualitative behaviors could have been simulated as well even if X had been made a dependent variable by the stiff coupling of Eq. (4). We do not see how temporary bistability could have been modeled if semi-intermediate P had been eliminated as an independent variable in this model.

It is barely conceivable as a mathematical exercise that bursting (vii) could be simulated with only two independent variables, but all successful models have used more than that number. Deterministic chaotic behavior (viii) would certainly require more than two variables for any simulation.

However, our surprise is not that certain experimental behaviors are incapable of simulation with only two variables. Rather, we are impressed with how much can be done in the sections presented above. We have reported many things which are already known from previous studies, but we believe the quantitative description of two excitability limits has been new and that the arguments about other items get together in one place a description of the possible behaviors of a useful model for a remarkable chemical system.

ACKNOWLEDGMENTS

This work was supported in part by Grant No. CHE-8405518 from the National Science Foundation. This paper is No. 75 in the series "Chemical Oscillations and Instabilities." Number 74 is M. B. Rubin and R. M. Noyes, J. Phys. Chem. (in press). After a preliminary draft of this manuscript had been prepared, Professor John J. Tyson called our attention to Ref. 27 where many of our conclusions had been anticipated by analytical arguments.

APPENDIX A: NUMBER OF POSSIBLE STEADY STATES

When Eqs. (2) and (3) are simultaneously zero, we obtain

$$Z_{ss} = \frac{k_1 A Y_{ss} + k_2 X_{ss} Y_{ss}}{f k_5} = \frac{k_3 A X_{ss}}{k_5} . \tag{A1}$$

Combination with Eqs. (1) and (2) then leads to

$$Y_{ss} = \frac{f k_3 A X_{ss}}{k_1 A + k_2 X_{ss}} = \frac{k_3 A X_{ss} - 2k_4 X_{ss}^2}{k_2 X_{ss} - k_1 A} . \tag{A2}$$

Equation (A2) rearranges to Eq. (A3):

$$2k_2 k_4 X_{ss}^2 + [(f-1)k_2 k_3 + 2k_1 k_4] A X_{ss} - (f+1) k_1 k_3 A^2 = 0 . \tag{A3}$$

The Descartes rule of signs states that regardless of the value of f there is one and only one positive value of X_{ss} which is a root of Eq. (A3). That value uniquely defines Y_{ss} and Z_{ss} by means of Eq. (A2) and (A1), respectively. Therefore, for any set of positive values of f, A, and k_1–k_5, there is one and only one steady state in the positive quadrant of the YZ plane or in the positive octant of XYZ space.

Once X_{ss} has been computed from quadratic Eq. (A3), the desired point in the YZ plane can be obtained from Eq.

(A1) and (A2). The conclusion is similar to one reached for the three-variable Oregonator by Tyson in Chap. III of Ref. 26.

APPENDIX B: APPROXIMATE EQUATIONS FOR NULLCLINES

All numerical values in this Appendix and Appendix C are based on the parameter assignments of Table I.

The curves in Fig. 1 can be approximated very well by noting there is an almost discontinuous change in behavior whenever Y passes through Y_{crit} given by

$$Y_{\text{crit}} = k_3A/k_2 = 5\times10^{-7}. \tag{B1}$$

The following approximate equations are valid to very good accuracy whenever Y deviates from Y_{crit} by more than about 10^{-9}.

When $Y < Y_{\text{crit}}$, Eqs. (1)–(4) lead to Eqs. (B2)–(B4). The arrows indicate limiting values at small Y:

$$X_\beta = \frac{k_3A - k_2Y}{2k_4} = 10^{-5} - 20Y \rightarrow 10^{-5}, \tag{B2}$$

$$Z(Z_{\text{null}}) = k_3AX_\beta/k_5 = 10^{-2} - 2\times10^4Y \rightarrow 10^{-2}, \tag{B3}$$

$$Z(Y_{\text{null}}) = \frac{k_2X_\beta Y}{fk_5} = \frac{2\times10^4Y - 4\times10^{10}Y^2}{f} \rightarrow 2\times10^4Y/f. \tag{B4}$$

The Y nullcline will reach a local maximum (designated M in Fig. 1) when

$$Y_M = 2.5\times10^{-7}, \tag{B5}$$

$$Z_M = 2.5\times10^{-3}/f. \tag{B6}$$

Approximate Eqs. (B5) and (B6) are obtainable by differentiation of Eq. (B4) and are valid to better than four significant figures.

When $Y > Y_{\text{crit}}$, the behavior of the nullclines is described by Eqs. (B7)–(B9). The arrows indicate limiting values at large Y:

$$X_\alpha = \frac{k_1AY}{k_2Y - k_3A} = \frac{0.2Y}{2\times10^9Y - 1000} \rightarrow 10^{-10}, \tag{B7}$$

$$Z(Z_{\text{null}}) = \frac{200Y}{2\times10^9Y - 1000} \rightarrow 10^{-7}, \tag{B8}$$

$$Z(Y_{\text{null}}) = \frac{(k_1A + k_2X_\alpha)Y}{fk_5} \rightarrow Y/2.5f. \tag{B9}$$

The local minimum in the Y nullcline (designated N in Fig. 1) occurs when

$$Y_N = 8.535\times10^{-7}, \tag{B10}$$

$$Z_N = 5.828\times10^{-7}/f. \tag{B11}$$

APPENDIX C: TRAJECTORIES OF STABLE LIMIT CYCLES

The approximate equations for the nullclines from Appendix B provide some simple and surprisingly accurate estimates of the trajectories and periods of a limit cycle.

Equations (B2)–(B4) will be appropriate for points to the left of line C in Fig. 2, and Eqs. (B7)–(B9) will be appropriate to the right of that line.

The calculation of a trajectory can start on line C near point M where it will be a good approximation to assume the value of Z is given by Eq. (B6). From that point until the trajectory again intersects line C near point N, X can be approximated by the limiting value for X_α in Eq. (B7), and Eqs. (2) and (3) reduce to

$$\frac{dY}{dt} = fk_5Z - 2k_1AY, \tag{C1}$$

$$\frac{dZ}{dt} = -k_5Z. \tag{C2}$$

If τ is time after the start of such a trajectory, and if Y has had time grow much larger than Y_{crit}, these linear equations generate

$$Z_\tau = Z_Me^{-k_5\tau}, \tag{C3}$$

$$Y_\tau = \frac{fk_5Z_M}{2k_1A - k_5}[e^{-k_5\tau} - e^{-2k_1A\tau}]. \tag{C4}$$

If t_{MP} is the time to move from line C near point M to the maximum Y at point P, Eq. (B9) generates

$$Y_P = \frac{fk_5Z_M}{2k_1A}e^{-k_5t_{MP}}. \tag{C5}$$

Equations (C3)–(C5) can be solved simultaneously to obtain the three quantities Y_P, Z_P, and t_{MP}. The time t_{MN} for the transition from line C near M to line C near N can be calculated by substitution of Y_{crit} into Eq. (C4). The results of these approximate calculations are compared in Table III to the numbers obtained by an exact trajectory integration for $f = 1$.

For the transition from the start of the trajectory to maximum Y at point P, the coordinates of that point and the time to attain it are reproduced to within about 1%. The major part of a period involves the passage to the right of Y_{crit}, and the approximate equations reproduce this time to within better than 4%.

For the remainder of the trajectory from line C near point N to line C near point M, the k_1AY term in Eq. (2) can be neglected. For this trajectory, we can use the approximation $X = k_3A/2k_4$ as the limiting value from Eq. (B2). Then Eqs. (2) and (3) reduce to

$$\frac{dY}{dt} = fk_5Z - k_2XY, \tag{C6}$$

$$\frac{dZ}{dt} = k_3AX - k_5Z. \tag{C7}$$

If τ is time after the start of such a trajectory, and if Z has had time to grow much larger than its initial value, these

TABLE III. Comparison of approximate and exact calculations for trajectories between Y_{crit} values when moving from near M to near N.

Quantity	Approximate Eqs. (C3)–(C5)	Exact integration at $f = 1$
Y_P	1.357×10^{-3}	1.363×10^{-3}
Z_P	$5.429\times10^{-4}/f$	5.364×10^{-4}
t_{MP}	1.527	1.544
t_{MN}	22.57	21.75

TABLE IV. Comparison of approximate and exact calculations for trajectories between Y_{crit} values when moving from near N to near M.

Quantity	Approximate Eqs. (C8) and (C9) $f=0.505$	$f=1.000$	$f=1.940$	Trajectory integration for $f=1$
Y_Q	1.3×10^{-10}	2.5×10^{-10}	4.8×10^{-10}	2.6×10^{-10}
Z_Q	5.3×10^{-6}	5.0×10^{-6}	4.6×10^{-6}	5.5×10^{-6}
t_{NQ}	0.000 53	0.000 50	0.000 46	0.0009
t_{NM}	0.68	0.29	0.14	0.44

linear equations generate

$$Z_\tau = (k_3AX/k_5)(1-e^{-k_5\tau}), \tag{C8}$$

$$Y_\tau = Y_{crit}e^{-k_2X\tau} + (fk_3A/k_2)(1-e^{-k_2X\tau}) + [fk_3AX/(k_2X-k_5)](e^{-k_5\tau}-e^{-k_2X\tau}). \tag{C9}$$

The most effective procedure for computation was to find t_{NQ} as the time when Y_τ went through a minimum at point Q and thus to obtain values for Y_Q and Z_Q. Those values satisfied Eq. (B4) just as they should.

To estimate the total time t_{MN} to go from line C near point N to line C near point M, Z_M from Eq. (B6) was substituted into Eq. (C8). Table IV shows the results of these approximate calculations for three values of f and compares the results with the trajectory integration for $f=1$.

The percentage deviations in Table IV are greater than those in Table III, but absolute times for this portion of the trajectory are so short that for $f=1$ the total period of the limit cycle based on the approximate equations differs by only about 2.5% from the value obtained by exact integration.

Tyson[27] used much the same equations to develop expressions for the slow portions of the relaxation oscillations but did not make a direct comparison of the total periods estimated analytically with those obtained by numerical integration of the equations of motion.

[1]R. J. Field and R. M. Noyes, Faraday Symp. Chem. Soc. **9**, 21 (1974).
[2]P. Ruoff, Chem. Phys. Lett. **90**, 76 (1982).
[3]P. Ruoff and R. M. Noyes, J. Phys. Chem. **89**, 1339 (1985).
[4]P. Ruoff and R. M. Noyes, J. Chem. Phys. **84**, 1413 (1986).
[5]Z. Noszticzius, M. Wittmann, and P. Stirling, J. Chem. Phys. **86**, 1922 (1987).
[6]This paper neglects the possibility of deterministic chaos, which would not be possible in the two-dimensional plane with which we shall be mostly concerned.
[7]J. Rinzel and W. C. Troy, J. Chem. Phys. **76**, 1775 (1982).
[8]W. C. Troy, *Oscillations and Traveling Waves in Chemical Systems*, edited by R. J. Field and M. Burger (Wiley, New York, 1985), pp. 145–170.
[9]R. J. Field and R. M. Noyes, J. Chem. Phys. **60**, 1877 (1974).
[10]Tyson (Ref. 11) has chosen for mathematical reasons to use the alternative approximation that $dY/dt=0$. We select the approximation of Eq. (4) because Y and Z are the quantities which can be determined independently by direct measurement.
[11]J. J. Tyson, J. Phys. Chem. **86**, 3006 (1982).
[12]R. M. Noyes, Ber. Bunsenges. Phys. Chem. **89**, 620 (1985).
[13]R. J. Field and H.-D. Försterling, J. Phys. Chem. **90**, 5400 (1986).
[14]J. J. Tyson, *Oscillations and Traveling Waves in Chemical Systems*, edited by R. J. Field and M. Burger (Wiley, New York, 1985), pp. 93–144.
[15]R. D. Janz, D. J. Vanecek, and R. J. Field, J. Chem. Phys. **73**, 3132 (1980).
[16](a) J. Maselko, Chem. Phys. **67**, 17 (1982); (b) **78**, 381 (1983); (c) J. Maselko and I. R. Epstein, J. Phys. Chem. **88**, 5305 (1984).
[17]Z. Noszticzius, P. Stirling, and M. Wittmann, J. Phys. Chem. **89**, 4914 (1985).
[18]V. Gaspár and P. Galambosi, J. Phys. Chem. **90**, 2222 (1986).
[19]"Entities are not to be multiplied without necessity," William of Ockham (1300?–1349?).
[20]K. Showalter, R. M. Noyes, and H. Turner, J. Am. Chem. Soc. **101**, 7463 (1979).
[21]A. T. Winfree, *Oscillations and Traveling Waves in Chemical Systems*, edited by R. J. Field and M. Burger (Wiley, New York, 1985), pp. 441–472.
[22]M. Marek and I. Stuchl, Biophys. Chem. **3**, 245 (1975).
[23]K. Bar-Eli and S. Reuveni, J. Phys. Chem. **89**, 1329 (1985).
[24]M. F. Crowley and R. J. Field, J. Phys. Chem. **90**, 1907 (1986).
[25]P. De Kepper and K. Bar-Eli, J. Phys. Chem. **87**, 480 (1983).
[26]J. J. Tyson, *Lecture Notes in Biomathematics. 10. The Belousov–Zhabotinskii Reaction* (Springer–Verlag, Berlin 1976).
[27]J. J. Tyson, J. Chem. Phys. **66**, 905 (1977).
[28]B. D. Hassard, N. D. Kazarinoff, and V.-H. Wan, *Theory and Applications of Hopf Bifurcation*, London Mathematical Society Lecture Notes Series No. 41 (Cambridge University, Cambridge, 1981).